Fluid-induced particle-size segregation in sheared granular assemblies

Sitangshu Bikas Santra,[1] Stefan Schwarzer,[1,2,*] and Hans Herrmann[1,2]
[1]*Laboratoire de Physique Mécanique des Milieux Hétérogènes, Ecole Supérieure de Physique et Chimie Industrielles, 75231 Paris, Cedex 05, France*
[2]*Institut für Computeranwendungen, Universität Stuttgart, Pfaffenwaldring 27, 70569 Stuttgart, Germany*
(Received 11 March 1996; revised manuscript received 20 June 1996)

We perform a two-dimensional molecular-dynamics study of a model for bidisperse granular systems under conditions of simple shear flow. We find that if the ratio of shear rate to viscosity is small, then the particles in the system arrange themselves in bands of big and small particles oriented along the direction of the flow. Each band contains particles of one species only. We present a mechanism for this particle-size segregation phenomenon based on the observation that segregation occurs if the viscous length scale introduced by a liquid in the system is smaller than the mean free path of the particles. For large values of shear rate to viscosity the system remains disordered. [S1063-651X(96)05211-7]

PACS number(s): 47.55.Kf, 83.20.Hn, 02.70.Ns

I. INTRODUCTION

If a mixture of particles and liquid is sheared, either in a continuous fashion or by periodic excitation of the system, a host of structural rearrangements in the mixture are known to occur. Most of the systems studied experimentally involve monodisperse suspensions [1–3]. For concentrated suspensions and oscillatory shearing, the formation of layers in the isovelocity planes and an additional arrangement in lines of particles perpendicular to the velocity field [3] has been observed. In addition, simulations of Taylor-Couette flow in the viscous regime confirm the organization of the suspended particles in layers oriented along the isovelocity planes [4]. The numerical studies have seen cluster formation within the formed planes. However, while for bidisperse suspensions similar organization patterns have been observed [3] in experiments and size-distribution induced instabilities are known to occur in sedimenting systems [5], simulations of bidisperse systems have not found so far clear indications of size segregation under shear.

In this paper, we simulate a sheared, bidisperse particle-liquid mixture in two dimensions. We find size segregation of this system for sufficiently low shear rates. We propose a segregation mechanism that depends on the presence of a viscous length scale in the system of the same order as the particle sizes. The mechanism is of rather general nature and may also apply to three-dimensional systems.

II. MODEL

We concentrate on laminar shear flows described by local shear rates $\dot{\gamma} \equiv (\partial/\partial y) v_x$. We have in mind (see Fig. 1) that the flow is translationally invariant in the x direction and that its speed varies linearly in the y direction. For the sake of simplicity we assume that the particle-size distribution is bidisperse. More precisely, our system consists of a number n_s of small and a number n_b of big disk-shaped particles with radii r_s and r_b, respectively. The overall area fraction c is the sum of the area fractions of big and small particles $c = c_s + c_b$.

If particles are immersed in viscous fluids and if the Reynolds number is low, then lubrication effects will introduce a strong velocity-dependent damping diverging as the surfaces of two particles approach each other. Effectively, no direct contact occurs between particles, but only a transfer of momentum that is strongest along the direction joining the particle centers. In our model we use, for simplicity, strong repulsive forces between overlapping particles and include a velocity proportional damping. In particular, along the direction joining two particle centers, we introduce a damped harmonic force f_n,

$$\frac{f_n}{\mu} = \begin{cases} -\xi + 2\kappa\dot{\xi} & \text{if } \xi > 0 \\ 0 & \text{otherwise,} \end{cases} \tag{1}$$

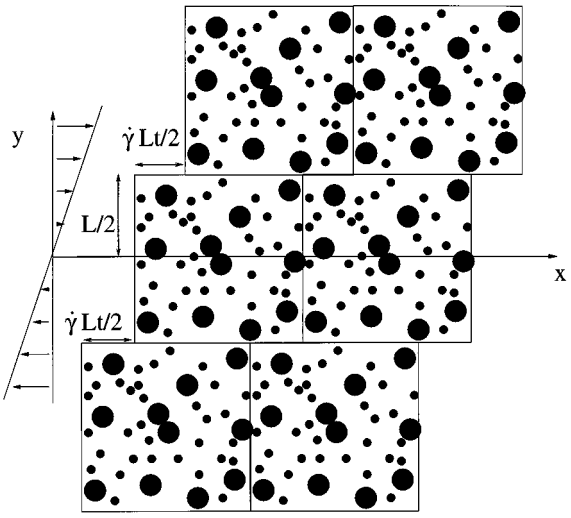

FIG. 1. Sketch of the model geometry for shear flow. The simulation cell of size $L \times L$ is periodically repeated in the x direction. The cell images in the $\pm y$ directions are shifted by an amount $\pm \dot{\gamma} L t/2$ to reflect the particle displacement at the top and bottom of the cell, which grows linearly in time due to the shear (Lees-Edward boundary conditions).

*Electronic address: sts@ica1.uni-stuttgart.de

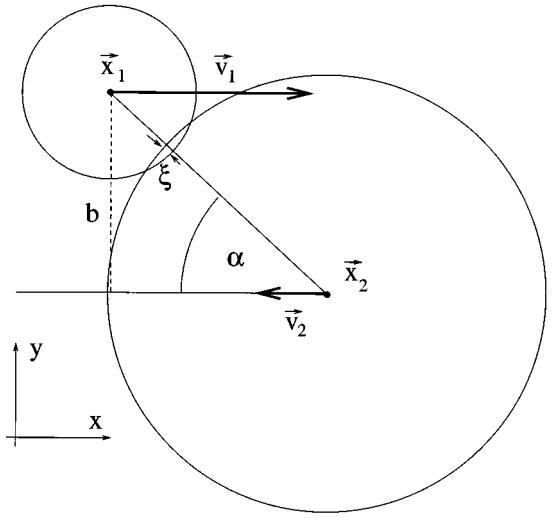

FIG. 2. Geometry of the collision between two disks in the center-of-mass frame. The particles are assumed to initially move parallel to the flow such that laboratory frame and center-of-mass frame are aligned.

where μ is the reduced mass of the pair, $\xi \equiv (r_1+r_2)-|\mathbf{x}_1-\mathbf{x}_2|$ is the virtual overlap of the two particles located at $\mathbf{x}_1$ and $\mathbf{x}_2$ (Fig. 2), and κ parametrizes a damping proportional to the velocity. This harmonic force (1) is purely repulsive and forces act only if there is an overlap of the particle pair.

The form of Eq. (1) is such that the *restitution coefficient* e, the ratio of the normal velocities after and before the impact, is the same for all binary collisions, independent of mass and velocity. The restitution is related to κ by $\kappa \equiv 1/\sqrt{1+[\pi/\ln(e)]^2}$. In order to mimic the dissipative effects of the lubrication forces, we have chosen in this work $e=0.8$, which is still in the range of typical materials in air ($e \approx 0.92$ for steel or ≈ 0.6 for aluminum beads). Equation (1) is in dimensionless form. The chosen length scale is the average radius $\overline{r} \equiv (n_b r_b + n_s r_s)/(n_b+n_s)$, the mass unit is the mass of a particle of average radius, and the time unit is such that the duration of a pair contact, half the period of a damped harmonic oscillator, becomes π for vanishing damping $\kappa \to 0$. In these units the spring constant of a pair interaction does not appear in Eq. (1) since $\sqrt{k/\mu}=1$.

Since we have neglected tangential forces in our model we do not consider rotational degrees of freedom. However, as will become clear in the discussion in Sec. III, we believe that rotation does not play an essential role for the physics of our model.

We approximate the liquid motion by imposing an invariant, fixed-velocity profile pointing in the x direction [6],

$$\mathbf{u}(y) = y\dot{\gamma}\mathbf{e}_x, \tag{2}$$

where y is counted from the center of the simulation cell (cf. Fig. 1). The liquid exerts an additional viscous drag on each particle i, which is added to the interaction force (1) between particles. The force is here assumed to be the Stokes drag force on a sphere,

$$\mathbf{f}_{d,i} = -6\pi r_i \eta[\mathbf{v}_i - \mathbf{u}(y_i)], \tag{3}$$

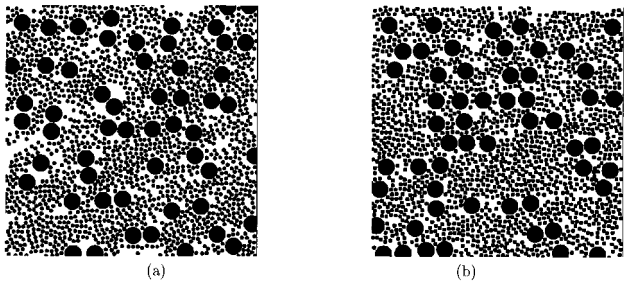

FIG. 3. Simulation snapshots at dimensionless time $\dot{\gamma}t=0$ (a) and 195 (b). The dimensionless shear rate in this system is $\dot{\gamma}=0.01$ and the viscosity $\eta=0.001$.

where $\mathbf{v}_i$ is the velocity of particle i, y_i its y coordinate, and η the viscosity of the liquid, measured in the time, length, and mass units given above.

The equations of motion are integrated using a fourth-order Gear predictor-corrector algorithm [7], with the time step chosen to be 0.15. We have tested the algorithm using this value of the time step for the case $\eta=0$ and $e=1$ and found good energy conservation.

To prepare the initial configuration, we start from a random, overlapping configuration of disks and simulate with periodic boundary conditions until time $t=20$ using a very low restitution coefficient of 0.1. During this period, particle overlaps are removed and the large excess energy due to the initial overlaps in the system is efficiently dissipated. Afterward the setup is continued with $e=1$ until $t=100$, corresponding to elastic collisions. The average energy per particle in the system during this stage is quite low and allows only marginal overlaps. Since no shear is applied in this stage and the system responds elastically, the resulting configurations have statistical weights close to those of an equally dense hard-disk system.

Before finally switching over to a simulation with restitution coefficient $e=0.8$ including the shear due to the background velocity profile, the particle velocities are reassigned such that the particles initially rest with respect to the local liquid-background velocity field [Eq. (2)]. The boundary conditions for the particles are Lees-Edwards boundary conditions (as displayed in Fig. 1, cf. also [7]).

Since the system is sheared and x momentum is transported in the y direction by particle collision, we do work on the system and it would continuously heat up if there were no energy sinks available. However, there are two sources of energy dissipation in the system: on the one hand, the inelastic particle collision dynamics and, on the other hand, the viscous drag exerted by the liquid. These serve as sinks for the work done on the system. Thus we do not require a thermostat as in Hamiltonian nonequilibrium molecular dynamics. However, one may define a ''local temperature'' of the system by studying the excess velocities of the particles as compared to the constant velocity field of the liquid background. We will revisit this question below.

III. RESULTS AND DISCUSSION

In Figs. 3 and 4 we show two typical simulation sequences whose physical parameters differ only in the value

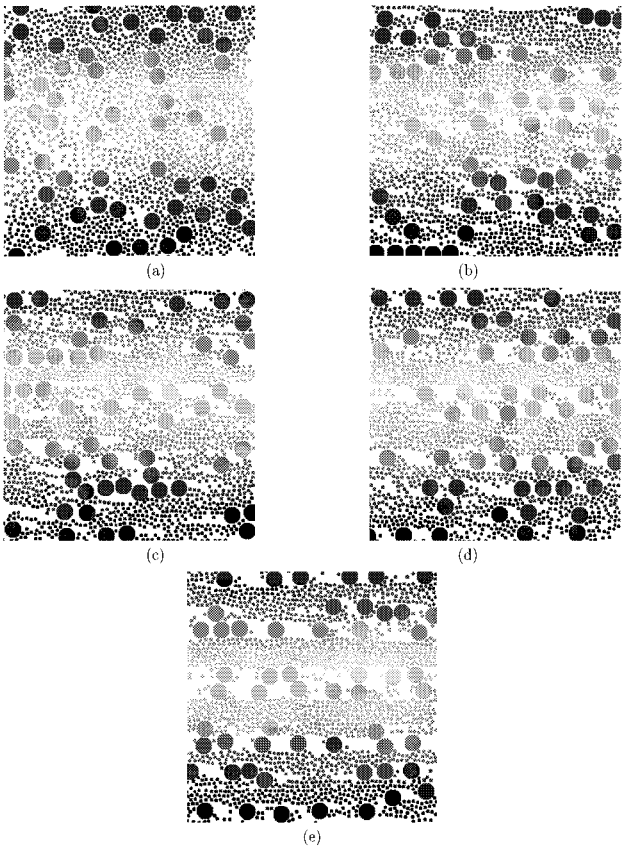

FIG. 4. Simulation snapshots at dimensionless time $\dot{\gamma}t=0$ (a), 20 (b), 70 (c), 110 (d), and 220 (e). The dimensionless shear rate in this system is $\dot{\gamma}=0.01$ and the dimensionless viscosity $\eta=0.01$, ten times larger than in Fig. 3. Different shades of gray indicate the modulus of the x velocity of the particles.

for the background viscosity η. The ratio of the particle radii in our bidisperse system is $r_b/r_s=4$, the ratio of the number density of big and small particles is $n_b/n_s=0.05$, and the total area fraction of particles is rather high, $c=0.6$. In the long-time limit one sees very different structural reordering of the systems emerging. In the first sequence (Fig. 3) with low viscosity, the particle arrangement is more or less random, whereas in the second case (Fig. 4) one observes a very clear separation into alternating zones parallel to the flow direction that contain alternating big and small particles.

The basis to understand this segregation phenomenon lies in an analysis of the length scales that are present in the system. Apart from the system size and the two different particle radii, an additional viscous length exists in the problem. Given that a particle has a typical particular velocity against the liquid background of $\mathbf{v}_0$, which it acquires in collisions (see below), the viscous length ζ is the typical distance that a particle has to travel before it again acquires the velocity of the background. The length ζ may be estimated in the following way. From the equations of motion $\mathbf{f}_{d,i}=m_i\dot{\mathbf{v}}$, i.e.,

$$\dot{v}_y=-\frac{6\pi r_i\eta}{m_i}v_y, \tag{4}$$

we obtain a simple exponential decay of any excess residual y component of the velocity,

$$v_y(t)=v_0\exp\left[-\frac{6\pi r_i\eta}{m_i}t\right], \tag{5}$$

with a time constant $\tau=m_i/6\pi r_i\eta$. A typical excess velocity v_0 created by a collision of two particles 1 and 2 is $v_0\approx(\mu/m_i)(r_1+r_2)\dot{\gamma}$. The product

$$\zeta_1\approx v_0\tau=\mu(1+r_2/r_1)\dot{\gamma}/6\pi\eta \tag{6}$$

estimates the viscous length for particle of type 1 after a collision with a type-2 particle. The value of ζ_1 is largest for $r_2/r_1=r_b/r_s$ and we call it simply ζ in the subsequent text. A detailed discussion is presented in Appendix A.

Let us now discuss the effects that let arise the segregation process.

(a) The particles move on average with the velocity of the liquid background measured at their centers. The collisions between particles tend to drive the system to a disordered state [8]. The ratio of the viscous length to a typical interparticle distance is a measure of the efficiency of this process: the larger the viscous length, the more effectively a collision will disturb a possibly ordered state of the system.

(b) Conversely, however, in a highly viscous environment with $\zeta\ll 1$, the collisions between particles only weakly influence the spatial configuration of the system and order may be created.

These two observations show that the viscous length plays the central physical role in the segregation process. We will try in the following to obtain a better understanding by identifying possible stationary states of the systems and their stability to perturbations.

A. Stationary states of monodisperse systems

To this end let us first consider possible stationary (collisionless) states of a monodisperse system of particles with radius $r=1$. Each single particle defines, due to its finite extension, a horizontal ''lane'' in the system, i.e., the area that it would cover as time passes if no other particles were present in the system.

To avoid collisions, either (i) two particles have to be separated in the y direction by more than $2r$ or (ii) there may not be a difference in the y position of the two particles' centers since then the friction with the liquid background will equalize their velocities. For a finite system of given height h and width w one can find a maximum particle concentration $(h/2r)(\pi r^2/hw)=(\pi r/2w)$, above which not all particles can be in different and disjoint lanes [condition (i)], thus leading (trivially) to a stationary state. However, for an infinite system this concentration threshold tends to zero and collisions will necessarily occur if the particles are positioned randomly. The only possible stationary states at nonzero concentration are thus lanes or ''strings'' of particles with the same y coordinate aligned along the x direction. If the x separation between particles in one lane is 0 and likewise the separation between lanes vanishes, then the packing fraction of particles is the largest, consistent with a collisionless stationary state of the system. The maximum possible

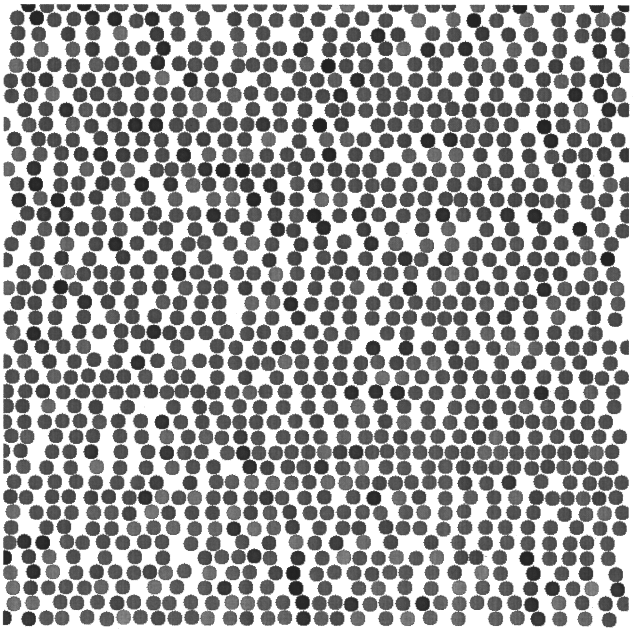

FIG. 5. Final state of the simulation of a monodisperse system with dimensionless shear rate $\dot{\gamma}=0.01$ and dimensionless viscosity $\eta=0.01$, equal to the values in Fig. 4. Different shades of gray denote different excess velocities with respect to the viscous background. Most particles of the system move with the background velocity; only in a few regions do we still see increased excess velocities indicating recent pair encounters.

density associated with such a state is $c_0 \equiv \pi/4 \approx 0.78$. We perform our simulations at $c=0.60$ and are well below this limit.

Such a particle arrangement in disjoint lanes is highly singular, but under certain conditions it is stable against perturbations. Let the vertical distance between lanes be small with respect to the particle radius and imagine one particle in one of the lanes being slightly displaced in the $+y$ direction. The particle will either undergo a collision with another particle in the lane above, which will then reduce its y coordinate again, or collide with a particle in its own lane, increasing the original displacement. If the viscous length ζ is large ($\gg r$), this collision typically displaces both collision partners to the other lane (if at the same time also the mean free path is large enough; see Appendix B). Thus, for $\zeta \gg r$, lanes are not stable and the system will not order.

In contrast, if ζ is small ($\ll r$), then the relative motion of the two particles is more akin to a sliding on top of each other, displacing each particle by approximately 1/2 in the $+y$ and $-y$ direction, respectively. In a sufficiently dense system subsequent collisions with particles in the neighboring lanes can then restore the original vertical positions of the particles: the system orders. In Fig. 5 we display the final state of the simulation of a monodisperse system with $\zeta \ll r$. All other simulation parameters equal those of Fig. 4. Very clearly, we observe the formation of disjoint parallel lanes of particles as explained above.

B. Stationary states of bidisperse systems

Let us now consider the bidisperse case. We can imagine that lanes consisting as well of big and small particles are stable. However, it is simple to see that this is not the case: If ζ is small in comparison to the big particle radius, then small particles in lanes containing big particles will be ejected from the big particle lane by collisions because the y positions of the particles always differ slightly. The reason for this ''snowplow'' behavior of the big species is that the big massive collision partner is not significantly displaced by one collision, whereas the small partner is. If then the neighboring lane contains small particles, it is not hard to absorb the additional expelled particle or to form an additional lane. If, however, the neighboring lane contains big particles, alternating collision series of the small particle with big particles below and above will establish an additional small particle lane in between the big particle lanes.

A typical simulation sequence of the ordering process at small ζ is displayed in Fig. 4. As explained above, we observe how the big particles act as plows and push the smaller particles aside. Thus the number of small particles in the big particle lanes decreases. Consequently, the collisions between small and big particles tend to drive the larger ones into lanes already occupied by large particles. Finally, lanes form according to the sizes of the constituents of the system.

C. An ''order parameter'' for size segregation

To arrive at a quantitative description of the segregation process, we define an ''order parameter'' in the following way. Since we have observed a strong stratification of the flow into horizontal layers, we define for each particle species the area fraction in a horizontal strip of width of the average particle radius. For a completely segregated system, we expect the area fraction of small particles c_s to be large whenever the fraction of big particles c_b is small. Consequently, the quantity

$$\delta \equiv \langle [c_b - c_s - \langle c_b - c_s \rangle]^2 \rangle^{1/2} \tag{7}$$

is small for a random mixture of the two species and assumes a large value when the system is stratified. The angular brackets denote the average over all examined horizontal slices.

In Fig. 6 we show the time dependence of δ for different values of ζ for constant overall area fraction $c=0.6$ and constant shear rate $\dot{\gamma}=0.01$. We clearly see an initially fast size segregation process that becomes slower and slower and finally saturates to a value δ_∞ that depends on ζ. Due to the rather low value of ζ and consequently a strong nonergodicity of our systems, the sample-to-sample fluctuations are large and values of $0.2\delta_\infty$ are typical in samples of size 100×100.

The decreasing dependence of δ_∞ on ζ, which demonstrates the mixing or destabilizing effects of large ζ, is shown in Fig. 7. The figure shows data obtained for different fluid viscosities and shear rates $\dot{\gamma}$, but constant overall area fraction. The scatter is rather large due to the above-mentioned sample-to-sample fluctuations. At large ζ, the segregation does not increase significantly over the initial value. In fact, if ζ is larger than the mean free path between particles, then the spatial distribution of particles does not differ much from that of the corresponding, inelastic, sheared hard-core gas [9–12]. However, at small ζ the friction with

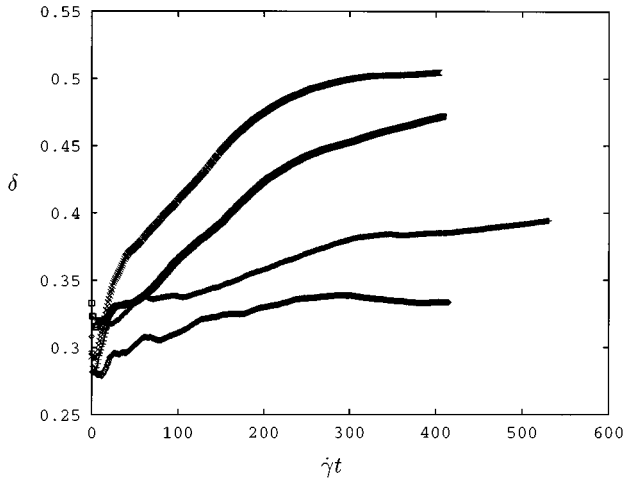

FIG. 6. Time dependence of the segregation parameter δ for simulations with different dimensionless viscosity $\eta=0.001$ (bottom), 0.004, 0.01, and 0.03 (top) corresponding to $\zeta\approx 2.5$, 0.63, 0.25, and 0.08 [according to Eq. (A6)] vs dimensionless time $\dot{\gamma}t$ on the abscissa.

the liquid is very large and we observe the ordering phenomenon described above. The data points in Fig. 7 result from runs to a time of $\dot{\gamma}t=1\,000$ by averaging δ over the last tenth of the simulation interval. We still observe a very slow systematic increase of δ with time for the highly viscous systems. However, we have estimated the systematic error of δ_∞ by two very long runs of $\dot{\gamma}t=2\,000$ for $\zeta=0.25$ to be about 7%. Thus its value lies within the range of the statistical error resulting from the system's memory of its initial configuration.

Figure 7 displays data for only one fixed particle concentration in the system. In Appendix B we discuss the dependence on particle concentration and how the concentration may be introduced into the scaling considerations above.

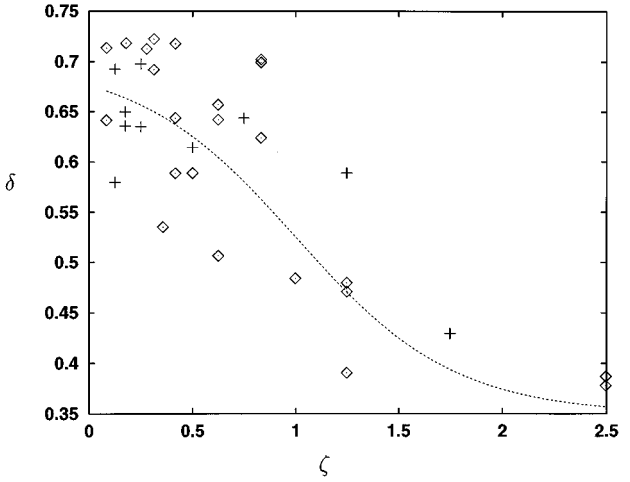

FIG. 7. Final values δ_∞ of the segregation parameter plotted vs viscous length ζ [according to Eq. (A6)] on the abscissa for several values of viscosity and shear rate in the system. Crosses denote computations with the constant viscosity $\eta=0.01$ and diamonds indicate the constant shear rate $\dot{\gamma}=0.01$.

IV. CONCLUSION

We have studied sheared bidisperse granular systems under conditions of simple shear flow. We find that the presence of the liquid can induce particle-size segregation. We propose as segregation criterion to consider the ratio of shear rate to viscosity. If this ratio is much less than 1 segregation occurs, if it is much greater than 1 there is no segregation. This statement is equivalent to saying that the viscous length in the system should be small when compared to a typical linear scale in the problem such as, e.g., the particle radius. The particles arrange themselves in bands moving with the flow that contain alternating big and small particles.

The proposed segregation mechanism relies on the presence of a liquid phase. It is thus very different from known mechanisms in dry granular media, where gravity-induced avalanches occur and separate particles species whose static angles of repose differ.

It should be very interesting to study the behavior of the system with more than two particle species or a whole continuum of species or the dependence on the particle radius ratio. Studies of the system behavior in Poiseuille flow [13–15] have shown interesting effects from the diversity of time scales presented by the spatial variation of its shear rate. Moreover, although we believe that similar effects will arise, simulations in three dimensions and quantitative comparisons to experiments are highly desirable.

ACKNOWLEDGMENTS

We would like to thank in particular Stephane Roux for valuable suggestions. St.S. thanks Wolfgang Kalthoff and Stefan Luding for discussions. We thank the Höchstleistungsrechenzentrum of the Forschungszentrum Jülich for computer time on their Paragon parallel computer. St.S. gratefully acknowledges financial support by NATO.

APPENDIX A: VISCOUS LENGTH

We obtain an estimate (when no further collisions occur) for ζ by integration of the equations of motion $\mathbf{f}_{d,i}=m_i\dot{\mathbf{v}}$. Taking the drag force from Eq. (3), we have obtained the y component of the equation of motion (4).

Relation (4) leads to a simple exponential relaxation of the initial excess velocity $v_y(0)$,

$$v_y(t)=v_y(0)\exp\left[-\frac{6\pi r_i\eta}{m_i}t\right]. \tag{A1}$$

In an analogous fashion, we obtain the expression for the x component,

$$\dot{v}_x=-\frac{6\pi r_i\eta}{m_i}\left[v_x-\dot{\gamma}\int_0^t dt' v_y(t')\right], \tag{A2}$$

which we can integrate by standard methods to find $v_x(t)$. We define the viscous length as the norm of the vector valued integral

$$\zeta = \left\| \int_0^\infty dt[\mathbf{v}(t) - \mathbf{u}(y(t))] \right\| \tag{A3}$$

and use the solutions of (4) and (A3) to obtain

$$\zeta = \frac{m_i}{6\pi r_i \eta} \left\| \begin{pmatrix} v_x(0) - \dfrac{\dot\gamma m_i v_y(0)}{6\pi r_i \eta} \\ v_y(0) \end{pmatrix} \right\|. \tag{A4}$$

We then find typical values for $\mathbf{v}_0$ by a consideration of a two particle collision, say, between particles with label 1 and 2, assuming that the initial velocities equal $\mathbf{v}_i = \mathbf{u}(y_i)$ according to their different y positions in the flow (for a more complete discussion of inelastic two particle collisions, see, e.g., [16]). The velocities after the collision, in the reference frame comoving with the liquid at the initial position of particle 1, are

$$\mathbf{v}_1(0) = -\frac{\mu}{m_i} b\dot\gamma \begin{pmatrix} \sin\alpha \cos\alpha(1+e) \\ \sin^2\alpha - e\cos^2\alpha + 1 \end{pmatrix}. \tag{A5}$$

Here b denotes the impact parameter and $\sin\alpha \equiv b/(r_1+r_2)$; cf. Fig. 2. Thus, apart from order-one geometrical factors and some e dependence, the velocity of the scattered particle is [17] approximately equal to $(\mu/m_i)(r_1+r_2)\dot\gamma$. Therefore, ζ becomes largest for the small particles after a collision involving a big and a small particle:

$$\zeta \approx \frac{\mu(1+r_b/r_s)\dot\gamma}{6\pi\eta}. \tag{A6}$$

APPENDIX B: AN ESTIMATE FOR THE MEAN FREE PATH IN THE MONODISPERSE SYSTEM

The ratio of the viscous length to the mean free path of the particles in a nonviscous environment is probably an important dynamical characteristic of the system. If the mean free path is much shorter than the viscous length, the additional background viscosity will not have a big effect. If, on the other hand, the mean free path is much longer than the viscous length, then the behavior of the system is viscosity dominated. Here we would like to give an estimate of the mean free path in a monodisperse system for particles moving in the vertical direction. To allow for a simple calculation in the stationary situation, we resort to a simple hypothesis for the system's configuration at large times: due to the initial disorder the system arranges itself such that the number of horizontal particle lanes is maximum.

We note that under these circumstances the average horizontal distance d between two particles is set by the packing fraction. If the number of lanes is maximum, their width must be the smallest possible, namely, $2r$. One particle covers an area of πr^2 within the available area $2rd$. Consequently, the overall area fraction is

$$c = \frac{\pi r^2}{2rd} = \frac{1}{2}\pi\frac{r}{d}. \tag{B1}$$

As in Appendix A, we now assume that we perturb the trajectory of one particle by giving it a vertical velocity of order $r\dot\gamma$, which is of the same order as the velocity difference between two lanes $2r\dot\gamma$. If $d = 2r$, the system will not allow particles to penetrate into the neighboring lane. This situation is the densest packing compatible with a stationary state of the system, $c_0 = \pi/4$. As long as $d < 4r$ or, equivalently, $c > c_1 = \pi/8$, a particle will only occasionally be able to pass a lane. Considerations of the particle geometry aside, the probability for a hit should be proportional to the time spent in the lane by the scattered particle divided by the average time between the pass of two successive particles in the neighbor lane. The mean free path ℓ is given by the condition that this ratio be about 1, i.e.,

$$1 \approx \frac{\ell/\dot\gamma r}{(d-2r)/2\dot\gamma r} \tag{B2}$$

or

$$\ell/r \approx (d-2r)/2r = \frac{1}{4}\pi c^{-1} - 1 = \frac{c_0}{c} - 1. \tag{B3}$$

For even lower concentration, the particle has a good chance to pass one or even several lanes, each with probability $1 - p_{\rm hit} \approx 1 - [2r/\dot\gamma r]/[(d-2r)/2\dot\gamma r] = 1 - 2r/(d-2r)$. The probability to survive a distance x/r without hits is hence distributed exponentially,

$$p(x/r) \sim (1-p_{\rm hit})^{x/2r}, \tag{B4}$$

which yields, by normalization and determination of the expectation value,

$$\ell/r = -1/\ln(1-p_{\rm hit}). \tag{B5}$$

For small concentrations (and thus also small hitting probabilities) this equation may be expanded to yield the same form as (B3),

$$\ell/r \sim 1/p_{\rm hit} \sim \frac{c_0}{c} - 1. \tag{B6}$$

It is interesting to note that ℓ does not depend on the shear rate but only on geometrical properties of the system. This observation is in favor of our suggestion that the ratio of viscous length to particle radius ζ/r, as proposed in the main text and here in dimensional form, collapses the simulation data for δ at a fixed given c. If $\dot\gamma \ll 1$, we presume that ζ/ℓ may be a good scaling variable for varying area fractions. This may be an interesting question to investigate.

[1] B. Noetinger, L. Petit, E. Guazelli, and M. Clement, Rev. Phys. Appl. **22**, 1025 (1987).
[2] B. J. Ackerson and P. N. Pusey, Phys. Rev. Lett. **61**, 1033 (1988).
[3] P. Gondret, Ph.D. thesis, Université Claude Bernard, Lyon, 1994 (unpublished).
[4] G. Bossis and J. F. Brady, J. Chem. Phys. **80**, 5141 (1984).
[5] R. L. Whitmore, Br. J. Appl. Phys. **6**, 239 (1955).
[6] M. Doi and D. Chen, J. Chem. Phys. **90**, 5271 (1989).
[7] M. P. Allen and D. J. Tildesley, *Computer Simulations of Liquids* (Clarendon, Oxford, 1987).
[8] Goldhirsch and Zanetti [10] have studied in detail the particle distribution function in inelastic hard-disk systems. They have found that the particle distribution does not become truly random because clusters form. However, due to the shear applied to the system boundaries, these clusters are not stable but break up on a time scale related to the inverse shear rate.
[9] S. McNamara and W. R. Young, Phys. Fluids A **5**, 34 (1993).
[10] I. Goldhirsch and G. Zanetti, Phys. Rev. Lett. **70**, 1619 (1993).
[11] S. Luding, Ph.D. thesis, Albert-Ludwigs-Universität Freiburg, 1994 (unpublished).
[12] I. Goldhirsch and M.-L. Tan (unpublished).
[13] S. B. Santra, S. Schwarzer, and H. Herrmann (unpublished).
[14] S. Schwarzer, Phys. Rev. E **52**, 6461 (1995).
[15] W. Kalthoff, S. Schwarzer, G. Ristow, and H. Herrmann, Int. J. Mod. Phys. C **7**, 543 (1996).
[16] O. R. Walton, in *Particulate Two-Phase Flow*, edited by M. C. Roco (Butterworth-Heinemann, Boston, 1992), Chap. 25.
[17] We would like to point out that even in more elaborate models, which may include a more realistic rendering of the hydrodynamic interaction between the particles, the relevant velocity scale is of order $b\dot{\gamma}$, so that the subsequent arguments remain valid.